

## FPAA Implementations of Fractional-Order Chaotic Systems\*

**Kenan Altun**

*Department of Electronics and Automation,  
Vocational School of Technical Sciences,  
Sivas Cumhuriyet University,  
Sivas 58140, Turkey  
kaltun@cumhuriyet.edu.tr*

Received 29 September 2020

Accepted 16 April 2021

**Published 22 May 2021**

In this paper, fractional-order chaotic systems in an analog-based platform are realized using field programmable analog arrays (FPAA) hardware. With the help of this work, we aim to increase the complexity of chaotic systems. Approximated transfer functions in frequency domain are obtained by analyzing different values of fractional-order integrator with the Charef approximation method. In this study, fractional-order numerical calculation of Rssler and Sprott type-H chaotic systems is carried out. MATLAB Simulink model for chaotic systems that satisfy the conditions of chaos in the boundaries of fractional order value is schematically presented. Moreover, CAM designs and analysis that facilitate the realization of fractional-order transfer functions in FPAA platforms are introduced. The analog-based FPAA experimental and numerical outcomes for fractional order chaotic systems are demonstrated. The comparison of the results obtained in the numerical analysis and simulation study with the experimental results is given. This study confirms that the unpredictability of the chaos carrier signals realized by digital-based can be increased with analog-based FPAA hardware and fractional-order structures so as to provide safer transfer of information signals.

*Keywords:* Chaos; FPAA implementation; fractional-order chaotic system; nonlinear system.

### 1. Introduction

Chaos is the science that investigates the systems which exhibit irregular behaviors despite them having an order hidden in it. In the beginning of the 20th century, Henri Poincare, French mathematician, introduced the chaos theory. The chaos theory leads representing systems that exhibit irregular behaviors with simple dynamic equations.<sup>1</sup> Even though chaotic systems exhibit non-periodic behavior in the time domain, they show order in the phase space portrait. The chaotic signals are

\*This paper was recommended by Regional Editor Tongquan Wei.

characterized with non-periodic nature, sensitivity to initial conditions, wide-band structure, as well as their unpredictability in long periods.<sup>2</sup> These features of the chaotic signals scientifically contributed to solution of some problems.<sup>3</sup> The first application of chaos theory was initiated by Edward Lorenz in the 1960s.<sup>3</sup> The unpredictability of chaos signals in long periods has been used as a significant parameter in communication systems to improve their information security. As carrier signals, the chaos signals are the key components in the chaotic communication. The spread spectrum of chaos signals helps hide information signals in communication systems and ensure their arrival to receiver. Although the complexity of chaos signals increases the complexity of communication systems, they also improve the communication security. In other words, the characteristics of communication security amount to the predictability characteristics of chaotic signals. A nonlinear dynamic system that exhibits chaotic behavior has to contain at least one nonlinear term and three state variables in its equation set.<sup>4</sup> In these kind of nonlinear state equations, chaos conditions are generated by changing equation parameters and initial conditions. The nonlinear equation that is generated using fractional-order derivative operators does not require  $3^{rd}$  order state equation to provide chaos conditions. A dynamic system can exhibit chaotic behavior even in the case total order of the dynamic systems is less than 3.<sup>5</sup> This further complicates the predictability of chaotic systems. In fractional-order chaotic systems, existing parameters as well as the order of fraction as an additional parameter further increase the complexity of the chaotic systems.<sup>5</sup>

Even though the fractional-order derivative and integrator was first mentioned by Leibniz in 1695, their articulation was completed by Liouville and Riemann through the end of 19th century.<sup>6,7</sup> The fractional-order calculation contributed to full-fledged expression and solution of many problems in the field of electrical circuits, thermoelectric system, finance system, biological system.<sup>8</sup> In fact, many integer order models are the approximated version of the fractional-order model. The integer order model, however, cannot represent the nonlinear systems that are sensitive to initial and parameter values. The use of fractional order systems in nonlinear systems provided significant contribution to the design of electrical and control systems.<sup>9-14</sup> Fractional-order control systems, especially in nonlinear systems, lead to better system performance as compared to integer order control systems.<sup>15</sup> It can be also observed that the use of fractional-order operators helps modeling of problems in the nature and provide more precise results. *Dengue Fever* pandemic prevalence modeling using fractional order derivative facilitate the development of vaccine and treatment methods.<sup>5,16</sup>

The fractional-order derivative and integrators are described with many methods such as Grünwald–Letnikov’s (GL), Charef, Caputo and Riemann–Liouville (RL).<sup>20,17</sup> In the realization of fractional-order systems with discrete circuit components, researchers have experienced various difficulties due to selection and usage of active and passive circuit components. The existing methods mainly suffer from the fractional order chaotic systems sensitivity to (i) initial values, (ii) parameter

selections, and (iii) derivative degree. It is impossible to find a circuit element for the values determined in the resistor and capacitor selections for these designed structures. This limitation was further emphasized in Table 3 of the reference article i.e., finding circuit elements in the market with a precise value, e.g.,  $R = 504.48 \Omega$  and  $C = 21.78 \text{ nF}$  for  $q = 0.87$ . Furthermore, it is very difficult to repeat these operations for different dynamic systems and fraction degrees, e.g., for  $q = 0.88$ , all the values of circuit elements need to be calculated again. These difficulties bring field programmable gate arrays (FPGA) forward due to their advantages such as flexible usage and higher accuracy.<sup>21,18</sup> However, low sensitivity of digital-based systems because of rounding errors in long periods adversely affects the modeled system and ends up with misrepresentation of real system behavior.<sup>22–24</sup> It is impossible to fully observe Finite-precision arithmetic calculations in digital systems. Therefore, Pseudo(chaos)-orbits are eventually periodic and their cycle lengths may be rather short. Small rounding errors accumulate and cause large errors that lead to the reduced periodicity in dynamic systems. The errors that occur in each calculation step cause due to the lack of periodicity in dynamic systems and result in reliability issues in communication systems. The drawbacks of FPGA as well as the difficulties in the use of discrete circuit components make analog-based FPAA structures indispensable. The main disadvantage of this design is repetitive calculation of the fractional order values at the beginning of each design. On the other hand, these difficulties are easier to overcome while implementing the design and verifying the results via experiments as compared to the digital-based hardware and discrete circuit component designs.

In this paper, the aim is to carry out realization of the fractional-order chaotic signals using analog-based FPAA structures. The Charef approximation method is utilized to design fractional-order dynamic systems. The main purpose behind the use of fractional-order integrator is to reduce predictability of chaotic signals. Thus, chaotic signals can provide safer carrier signal to the communication systems.<sup>19</sup> Moreover, the use of analog-based FPAA structure is prioritized to obviate the predictable chaos signal problem that occurs in digital-based FPGA due to rounding errors in long periods.

The remainder of the paper is organized as follows. Section 2 mentions about Charef approximation method and gives the derivation of fractional orders. In Sec. 3, Rössler and Sprott type-H chaotic dynamics are modeled using Charef approximation method. Then, it compares the simulation results for different fractional-order chaotic systems. Section 4 includes the CAB design that is realized to implement fractional-order chaotic signals on an analog-based platform, and experimental results. Section 5 gives evaluations and conclusions.

## 2. Fractional Calculus

Fractional calculus is the integral pillar in system modeling, especially in the control systems.<sup>25–29</sup>

The fractional-order derivative with the order of 0.5 was first introduced by Leibniz and L'Hopital<sup>30,31</sup> to satisfy the scholarly curiosity: "Can the meaning of derivatives with integer order be generalized to derivatives with non-integer orders?"

The calculation of fractional order, however, requires a challenging and complicated process. In order to facilitate the process for analysis and simulations of control systems, the fractional-order operators are approximated to the integer order transfer functions. In the calculation of fractional-order derivative, fractional-order derivative operator acts like interpolation between neighboring integer derivatives. In the systems that calculate fractional-order derivative, the order of fraction as an additional parameter is used to better approximate complete system behavior. This feature of fractional order system provides significant contribution to nonlinear system modeling. Accordingly, researchers have developed many methods to approximate fractional order operators to the integer order transfer functions.<sup>32</sup>

The fractional order calculation is usually defined as (1). Herein,  $\alpha$  denotes the complex derivative or integral order.

$${}_a D_x^\alpha = \begin{cases} \frac{d^\alpha}{dt^\alpha}; & \text{Re}(\alpha) > 0 \\ 1; & \text{Re}(\alpha) = 0 \\ \int_a^t (d\tau)^{-\alpha}; & \text{Re}(\alpha) < 0. \end{cases} \quad (1)$$

In the following subsections, Riemann–Liouville approach along with Grünwald–Letnikov and Charef methods has been briefly explained as they are used in the study.

### 2.1. Riemann–Liouville

Riemann–Liouville is known as the most popular definition in the field of fractional analysis.<sup>33</sup> According to Riemann–Liouville definition, the mathematical expression of fractional-order integral equation is given as

$${}_a D_x^\alpha f(x) = \frac{1}{-\alpha} \int_a^x (x - \tau)^{-\alpha-1} f(\tau) d\tau, \quad \alpha < 0. \quad (2)$$

The  $n$ th order derivative of (2), when  $n - 1 < \alpha < n$ , is expressed as

$${}_a D_x^\alpha f(x) = \frac{1}{\Gamma(1 - \alpha)} \frac{d^n}{dx^n} \int_a^x (x - \tau)^{n-\alpha-1} f(\tau) d\tau, \quad n > 0. \quad (3)$$

Equation (3) amounts to  $(n - \alpha)^{th}$  power for the fractional order derivative of the function  $f(x)$ . Herein,  $a$  is the initial value while  $n$  is an integer number. Riemann–Liouville definition depends on the integral calculation of given function. Accordingly, fractional-order derivative is calculated using fractional-order integral and integer order derivatives.

**2.2. Grünwald–Letnikov**

Another popular definition used in the fractional analysis is proposed by Anton Karl Grünwald and Aleksey Vasilievich Letnikov<sup>11</sup> rather than the definition of Riemann–Liouville, Grünwald–Letnikov definition approach a problem with the basic derivative phenomenon. The basic derivative implies to the slope of a graph that is expressed by (4).

According to Grünwald–Letnikov definition, integro-differential equation with the order of  $\alpha$  is expressed as

$${}_a D_x^\alpha f(x) = \lim_{h \rightarrow \infty} \frac{\Delta_h^\alpha f(x)}{h^\alpha}, \tag{4}$$

where  $D$  is the differintegral operator and  $h$  is the number of step. The following equation gives the expansion of  $\Delta_h^\alpha f(x)$ :

$$\Delta_h^\alpha f(x) = \sum_{j=0}^{\infty} (-1)^j \binom{\alpha}{j} f(x - jh). \tag{5}$$

Equation (6) represents the case; summation calculation given in (5) is processed up to a finite number  $r$

$$\sum_{j=0}^r (-1)^j \binom{\alpha}{j} = \frac{1}{\Gamma(1 - \alpha)} \frac{\Gamma(r + 1 - \alpha)}{\Gamma(r + 1)}. \tag{6}$$

In Eq. (6),  $\Gamma(x)$  denotes the gamma function while  $h$  is its change in unit time and represented with  $h = \frac{(x-\alpha)}{r}$ . Finally, Grünwald–Letnikov definitio can be mathematically expressed as follows:

$${}_a D_x^\alpha f(x) = \lim_{r \rightarrow \infty} \left\{ \frac{\left(\frac{(x-a)}{r}\right)^{-\alpha}}{\Gamma(-\alpha)} \sum_{j=0}^{\infty} \frac{\Gamma(j - \alpha)}{\Gamma(j + 1)} f\left(x - j\left(\frac{(x-a)}{r}\right)\right) \right\}, \tag{7}$$

where  $\alpha$ ,  $a$  and  $\Gamma$ , respectively, denote a random number, initial value, Euler Gama function. In general,  $D$  is used to express both integrator and derivative. It should be noted that  $a$  is positive for derivatives whereas it is negative for integrators.

**2.3. Charef approximation method in frequency domain**

In this study, the aim is to carry out realization of the fractional-order chaotic signals using analog-based FPAA structures. In the design of FPAA, fractional- order derivative operators can only be modeled in frequency domain. In engineering, laplace and inverse laplace methods are used for linear system modeling in frequency domain. Among frequency domain modeling definition, Charef approximation is the most suitable method as it allows to obtain continuous approximation of fractional order system in s-domain.<sup>32</sup> With the help of this method, approximated integer

order transfer function of fractional order integral can be achieved within the specific interval of frequency and error rate.

$$I^{\alpha}(s) = \frac{1}{s^{\alpha}}, \tag{8}$$

where  $s = j\omega$  and  $\alpha$  stand for complex frequency and order of positive fractional integrator.

$$I^{\alpha}(s) = \frac{1}{s^{\alpha}} \approx \frac{1}{\left(1 + \frac{s}{p_T}\right)^{\alpha}}, \quad 0 < \alpha < 1. \tag{9}$$

In Eq. (9), in the calculation of the approximated transfer function,  $p_T$ ,  $p_0$ , and  $y$  denote corner frequency, first pole value, and error rate in dB. The last pole value,  $p_N$ , is determined by  $N$ .  $1/p_T$  represents the relaxation time constant. In the light of all these facts, fractional-order transfer function can be expressed as in the following equation:

$$I^{\alpha}(s) = \frac{1}{s^{\alpha}} \approx \frac{1}{\left(1 + \frac{s}{p_T}\right)^{\alpha}} \lim_{N \rightarrow \infty} \frac{\prod_{i=0}^{N-1} \left(1 + \frac{s}{z_i}\right)}{\prod_{i=0}^N \left(1 + \frac{s}{p_i}\right)}. \tag{10}$$

The poles and zeros of the transfer function are given as follows:

$$\begin{aligned} p_0 &= p_T 10^{[y/20\alpha]}, & z_0 &= p_0 10^{[y/10(1-\alpha)]}, \\ p_1 &= z_0 10^{[y/10\alpha]}, & z_1 &= p_1 10^{[y/10(1-\alpha)]}. \end{aligned} \tag{11}$$

Equation (12) describes the  $N - 1$  zero and  $N$  pole ratio.

$$z_{N-1} = p_{N-1} 10^{[y/10(1-\alpha)]}, \quad p_N = z_{N-1} 10^{[y/10\alpha]}. \tag{12}$$

Equation (13) provides the values of  $a$ ,  $b$  and  $ab$  that express the  $N - 1$  pole and  $N$  zero ratio.

$$a = 10^{[y/10(1-\alpha)]}, \quad b = 10^{[y/10\alpha]}, \quad ab = 10^{[y/10\alpha(1-\alpha)]}. \tag{13}$$

With the help of these explanations, the equation for the transfer function can be derived as

$$I^{\alpha}(s) = \frac{1}{s^{\alpha}} \approx \frac{1}{\left(1 + \frac{s}{p_T}\right)^{\alpha}} \approx \frac{\prod_{i=0}^{N-1} \left(1 + \frac{s}{z_i}\right)}{\prod_{i=0}^N \left(1 + \frac{s}{p_i}\right)} = \frac{\prod_{i=0}^{N-1} \left(1 + \frac{s}{(ab)^i a p_0}\right)}{\prod_{i=0}^N \left(1 + \frac{s}{(ab)^i p_0}\right)}. \tag{14}$$

Moreover, the dimension of the transfer function,  $N$ , can be found as

$$N = \text{int} \left( \frac{\log \left( \frac{\omega_{\max}}{p_0} \right)}{\log(ab)} \right) + 1. \tag{15}$$

With the help of Eqs. (14) and (15),  $s^\alpha$  value derived with Charef approximation method can be approximately obtained in the frequency domain within the interval of specific frequency and error rate.

### 3. Fractional-Order Chaotic Systems

As mentioned in the previous section, chaotic systems expressed with conventional calculation methods require at least 3rd dynamic representation. On the other hand, the fractional-order derivative is used to model a chaotic system with fractional-order system approximation. In this study, fractional order for MATLAB Simulink and analog-based FPAA is expressed in frequency domain using Charef approximation method. Fractional-order transfer function in frequency domain is obtained for Rössler and Sprott type-H chaotic system to be initially implemented in Simulink, then FPAA. To obtain transfer function, the eigenvalues of the dynamic system are calculated for the selected, minimum fraction order. The fraction order for every eigenvalue is obtained using Eq. (16). The greatest value among the obtained fractional order is selected as the fraction order of the system.<sup>34</sup>

In a dynamic system with the size of  $n$ , the eigenvalues,  $(\lambda_1, \lambda_2, \dots, \lambda_n)$ , are obtained using Jacobian matrices created for each dimension. Then, every single eigenvalue is used to determine the fraction order,  $\alpha$ , using (16), where  $q$  is expressed as the determined fraction order.

$$|\arg(\lambda_i)| > \alpha\pi/2, \quad \alpha = \max(q_1, q_2, \dots, q_n), \quad \forall(i = 1, 2, \dots, n). \quad (16)$$

If the given system is stable, fractional-order system is also stable at a point. In a condition that the given system is unstable, then the fractional-order system possibly exhibits chaos. The stability theorem for the fractional order systems is summarized in Fig. 1.

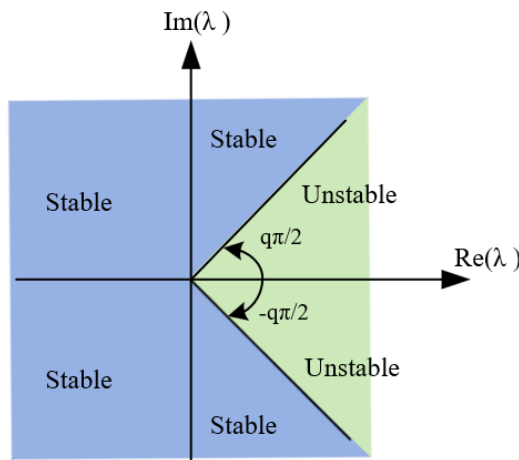


Fig. 1. Stability region of the fractional-order system.

Assume that the eigenvalues for the Jacobian matrix of a given fractional-order system are  $\lambda_1 = -1.7452$ ,  $\lambda_2 = 0.3476 + i2.2019$  and  $\lambda_3 = 0.3476 - i2.2019$ . In such a case, a fractional order needs to be calculated for the corresponding eigenvalue:  $\arg(\lambda_1) = \pi$ ,  $\arg(\lambda_2) = 1.41422$  and  $\arg(\lambda_3) = -1.41422$ . Then, fractional order using the expression  $\max(q_1, q_2, q_3)$  provides  $\alpha = q_2 = q_3 = 0.899$ . In the case  $q_1, q_2$  and  $q_3$  are greater than 0.899, all the equilibria of the (16) are unstable and dynamic system possibly exhibits chaos.

In the Charef approximation method, the fractional order for the given transfer function is determined as  $\alpha = 0.9$  in accordance with the literature. In this study, many fractional-order transfer functions used in simulation and experimental implementation are obtained using similar calculation method. For the approximated transfer function with the fraction order of  $\alpha = 0.9$ :  $\omega_{\max} = 100$  rad/s,  $y = 2$  dB,  $p_T = 0.01$  rad/s.

$$\begin{aligned}
 p_o &= p_T 10^{[y/20\alpha]} = 0.01 \cdot 10^{[2/20 \cdot 0.9]} = 0.0129, \\
 a &= 10^{[y/10(1-\alpha)]} = 10^{[2/10(1-0.9)]} = 100, \\
 b &= 10^{[y/10\alpha]} = 10^{[2/10 \cdot 0.9]} = 1.6681, \\
 ab &= 10^{[y/10\alpha(1-\alpha)]} = 10^{[2/10 \cdot 0.9(1-0.9)]} = 166.81.
 \end{aligned}$$

$$\begin{aligned}
 N &= \text{int} \left( \frac{\log \left( \frac{\omega_{\max}}{p_0} \right)}{\log(ab)} \right) + 1 = \text{int} \left( \frac{\log \left( \frac{100}{0.0129} \right)}{\log(166.81)} \right) + 1 \\
 &= \text{int} \left( \frac{3.889}{2.222} \right) + 1 = \text{int}(1.750) + 1 = 1 + 1 = 2.
 \end{aligned}$$

The values of  $a, b, ab$  are found with the transfer function that is generalized using the first pole value and (13). Afterward, the dimension of the transfer function is determined using (14). Finally, transfer function for the fraction order of  $\alpha = 0.9$  is obtained.

$$\begin{aligned}
 z_o &= p_0 10^{[y/10(1-\alpha)]} = 0,0129 \cdot 10^{[2/10(1-0.9)]} = 1.29, \\
 p_1 &= z_0 10^{[y/10\alpha]} = 1.29 \cdot 10^{[2/10 \cdot 0.9]} = 2.15, \\
 z_1 &= p_1 10^{[y/10(1-\alpha)]} = 2.15 \cdot 10^{[2/10(1-0.9)]} = 215.18, \\
 p_2 &= z_1 10^{[y/10\alpha]} = 215.18 \cdot 10^{[2/10 \cdot 0.9]} = 358.94.
 \end{aligned}$$

$$I^{0.9}_{(s)} = \frac{1}{s^{0.9}} \approx \frac{1}{\left(1 + \frac{s}{0.01}\right)^{0.9}} \approx \prod_{i=0}^1 \left(1 + \frac{s}{z_i}\right) \prod_{i=0}^2 \left(1 + \frac{s}{p_i}\right)$$



$$\begin{aligned}
 &= \frac{\left(1 + \frac{s}{(166.81)^0 \cdot 100.0 \cdot 0.0129}\right) \left(1 + \frac{s}{(166.81)^1 \cdot 100.0 \cdot 0.0129}\right)}{\left(1 + \frac{s}{(166.81)^0 \cdot 0.0129}\right) \left(1 + \frac{s}{(166.81)^1 \cdot 0.0129}\right) \left(1 + \frac{s}{(166.81)^2 \cdot 0.0129}\right)} \\
 &= \frac{\left(1 + \frac{s}{1.29}\right) \left(1 + \frac{s}{215.18}\right)}{\left(1 + \frac{s}{0.0129}\right) \left(1 + \frac{s}{2.15}\right) \left(1 + \frac{s}{358.94}\right)} = \frac{(1/p_T^\alpha)(0.036s^2 + 7.77s + 10)}{s^3 + 361s^2 + 776s + 10} \\
 &= \frac{(1/0.01^{0.9})(0.036s^2 + 7.77s + 10)}{s^3 + 361s^2 + 776s + 10} = \frac{63.095 \cdot (0.036s^2 + 7.77s + 10)}{s^3 + 361s^2 + 776s + 10} \\
 &= \frac{2.271s^2 + 490.24s + 630.95}{s^3 + 361s^2 + 776s + 10} .
 \end{aligned}$$

Equation (17) represents the fractional order,  $\alpha = 0.9$ , transfer function in frequency domain. This transfer function is used to design Simulink and FPAA CAM (Configurable Analog Module).

$$H(s) = \frac{\text{num}(s)}{\text{den}(s)} = \frac{2.271s^2 + 490.24s + 630.95}{s^3 + 361s^2 + 776s + 10} . \tag{17}$$

The transfer function of the system expresses the relation between input and output in frequency domain. Herein, the order of denominator should be greater than or equal to the order of nominator.

### 3.1. Rössler fractional-order chaotic attractor

The dynamic system belongs to Rössler chaotic generator, which is one of the chaotic oscillators obtained with fractional order analysis, as given in (18).<sup>35</sup> These chaotic system dynamic equations are composed of 3 dimensions and 6 terms.

$$\begin{aligned}
 D_t^{q_1} x(t) &= -y(t) - z(t) \\
 D_t^{q_2} y(t) &= x(t) + a.y(t) \\
 D_t^{q_3} z(t) &= x(t).z(t) - c.z(t) + b ,
 \end{aligned} \tag{18}$$

where  $q_1$ ,  $q_2$  and  $q_3$  are the order of fractional derivative.

In the given mathematical model,  $a = 0.20$ ,  $b = 0.20$  and  $c = 5.7$ , system parameters and the initial conditions for the chaotic system are given as  $x_0 = 0$ ,  $y_0 = 0$ ,  $z_0 = 0$ . Figure 2 represents the Rössler chaotic system Simulink design in which transfer functions are obtained using the calculation methods explained in the previous subsection. The eigenvalues of Rössler chaotic system’s Jacobian matrix for the initial conditions and parameters given above are  $\alpha_1 = -5.68718$ ,  $\alpha_2 = 0.0971028 + i0.995786$  and  $\alpha_3 = 0.0971028 - i0.995786$ .

In this case, the fractional orders need to be calculated for the corresponding eigenvalues derived as  $\arg(\lambda_1) = \pi$ ,  $\arg(\lambda_2) = 1.47359$  and  $\arg(\lambda_3) = -1.47359$ .

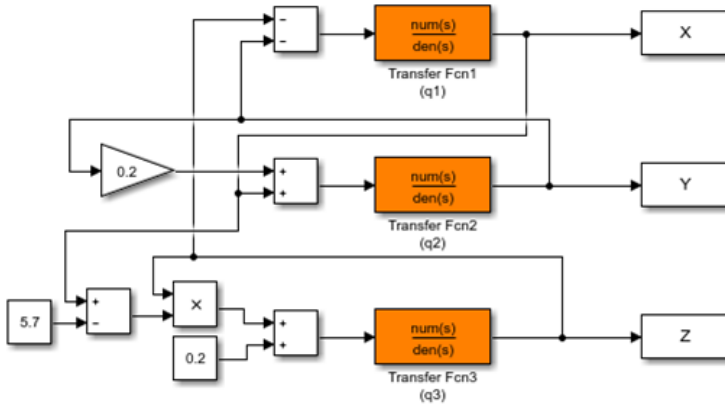


Fig. 2. Simulink model of fractional-order Rössler chaotic system.

Table 1. Chaotic attractors of the fractional-order Rössler chaotic system using the Charef method.

Fractional-order Values	x-y phase-space plots	x-z phase-space plots	y-z phase-space plots
$q_1 = q_2 = q_3 = 0.92$			
$q_1 = q_2 = q_3 = 0.94$			
$q_1 = q_2 = q_3 = 0.96$			
$q_1 = q_2 = q_3 = 0.98$			

Upon determining the fractional orders and with the help of the expression  $\max(q_1, q_2, q_3)$ ,  $\alpha = q_2 = q_3 = 0.9377$ . In this study, all the orders will be selected equivalent to each other and simulations will be realized in the order of 0.91–0.99. The outcome of the simulations is given in Table 1.

Table 1 represents that Rössler chaotic system with fraction order of 0.94 creates its first periodic window. It should be observed that Rössler chaotic system with a fractional order of 0.98 exhibits chaos. With the simulation study carried out here, the chaos state at fractional degrees calculated for the Rössler dynamic system was tested. It was shown that the chaotic behavior for the case is  $a = 0.98$ , where chaos conditions were theoretically confirmed so. Herein, the main purpose is to verify the theoretical results with the simulation outcomes.

### 3.2. Sprott type-H fractional-order chaotic attractor

In 1994, 19 nonlinear dynamic equations were recommended to produce complex chaotic signals and named A to S by Sprott. Among these systems, H system including one nonlinear term has six terms. State equations for the fractional order Sprott type-H system are given in the following equation<sup>35,36</sup>:

$$\begin{aligned} D_t^{q_1} x(t) &= -y(t) + z(t)^2 \\ D_t^{q_2} y(t) &= x(t) + 0.5y(t) \\ D_t^{q_3} z(t) &= x(t) - z(t), \end{aligned} \tag{19}$$

where  $q_1, q_2$  and  $q_3$  are the order of the fractional derivative. In the given mathematical model, the initial conditions for the chaotic system are given as  $x_0 = 0, y_0 = 0, z_0 = 0$ . Figure 3 represents the Sprott type-H chaotic system Simulink design.

The eigenvalues of Sprott type-H chaotic system’s Jacobian matrix for the initial conditions and parameters given above are  $\lambda_1 = -1, \lambda_2 = 0.25 + i0.968246$  and  $\lambda_3 = 0.25 - i0.968246$ .

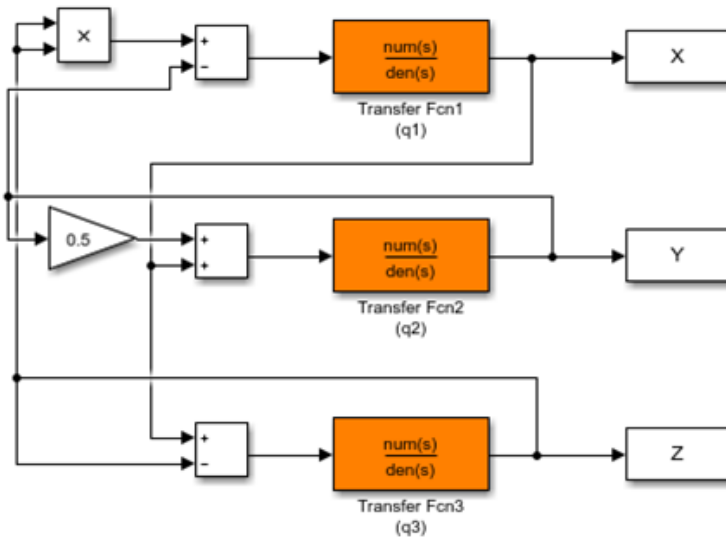
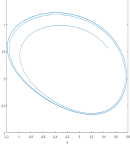
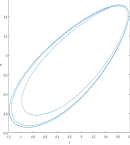
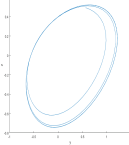
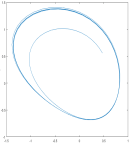
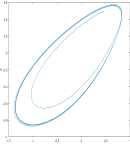
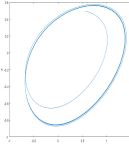
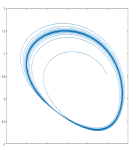
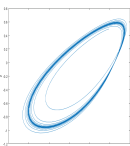
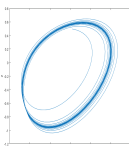
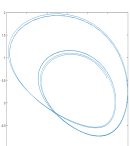
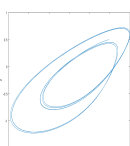
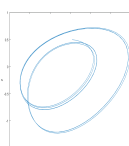
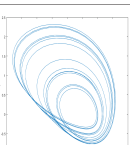
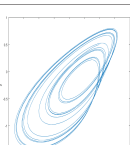
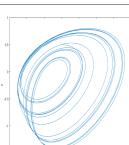
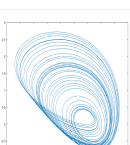
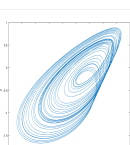
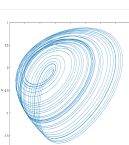


Fig. 3. Simulink model of fractional-order Sprott type-H chaotic system.

Table 2. Chaotic attractors of the fractional-order Sprott type-H chaotic system using the Charef method.

Fractional-order Values	x-y phase-space plots	x-z phase-space plots	y-z phase-space plots
$q_1 = q_2 = q_3 = 0.83$			
$q_1 = q_2 = q_3 = 0.85$			
$q_1 = q_2 = q_3 = 0.87$			
$q_1 = q_2 = q_3 = 0.89$			
$q_1 = q_2 = q_3 = 0.91$			
$q_1 = q_2 = q_3 = 0.93$			

In this case, the fractional orders need to be calculated for the corresponding eigenvalues derived as  $\arg(\lambda_1) = \pi$ ,  $\arg(\lambda_2) = 1.31812$  and  $\arg(\lambda_3) = -1.31812$ . Upon determining the fractional orders and with the help of the expression  $\max(q_1, q_2, q_3)$ ,  $\alpha = q_2 = q_3 = 0.9377$ . In this study, all the order will be selected equivalent to each other and simulations will be realized in the order of 0.80–0.93. The outcome of the simulations is given in Table 2.

Table 2 represents that Sprott type-H chaotic system with fraction order of 0.89 creates its first periodic window. It should be observed that Sprott type-H chaotic system with fraction order of 0.91 exhibits chaos. With the simulation study carried out, the chaos state at fractional degrees calculated for the Sprott type-H dynamic system was tested. It was observed that the system entered chaos for  $q = 0.91$ , where the theoretically calculated chaos conditions were met. Herein, the main purpose is to verify the theoretical results with the simulation outcomes.

Two distinct chaotic system simulations have been realized using the Charef approximation method. The following section presents the design of analog-based FPAA study for the order in which chaotic signals exhibit chaos.

#### 4. Experimental Realization of the Fractional-Order Chaotic Systems on FPAA

The use of discrete components in the design of electronic circuits is quite difficult, sometimes it is even impossible. Moreover, long required time to design circuit with discrete components and its ever increasing cost in the case of failures increase both the attention and research for programmable structures. However, analog-based circuit design could not provide promising performance since programmable structures are digital based. The drawbacks of analog-based systems such as rounding errors of decimally fractions and repetition of itself after a while make its utility reduced. Therefore, analog-based programmable structure comes forward. At the conclusion of rigorous research efforts, analog-based programmable FPAA structures have become available technology to verify and validate the design of circuits.<sup>37</sup> FPAA structures offer verification opportunity to the circuit designers such as high accuracy and low cost with user-friendly interface. FPAA structures can be used in the applications of analog-based systems, analog signal processing, biomedical sensor measurements, etc.<sup>38,39</sup> Among these applications, the attention on the design of chaos-based signal generators has a raising trend.<sup>40</sup> The investigation of chaos-based systems' dynamic equations shows that nonlinear circuit elements and passive circuit elements produced at the standard values have made the realization of chaotic systems quite difficult. Moreover, the difficulties in supplying these circuit elements prevent the experimental realizations of chaos-based studies. In the light of all these facts, FPAA structures provides easier programming, user-friendly interface, flexible work environment for the realization of chaos-based systems.<sup>41-43</sup>

FPAA development board consists of analog arrays that are configurable within 3.3–5 V. Figure 4 demonstrates the circuit structure used in this paper, Anadigm<sup>TM</sup> AN231K04-QUAD 3.3 V. FPAA is composed of configurable analog blocks (CAB) and programmable interconnection network. Moreover, it has configurable architecture in digital memory cells. On the other hand, CABs basically are the analog units that are composed of feedback opamps. In fact, a CAB is used to calculate some

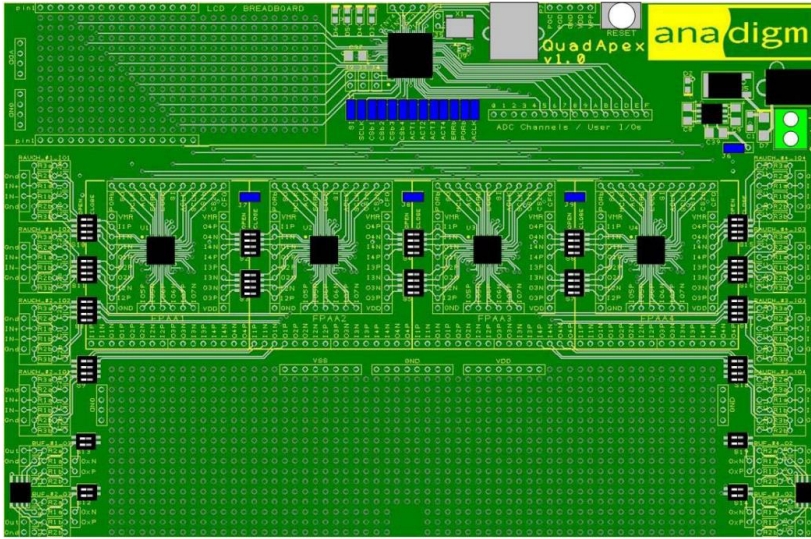


Fig. 4. Anadigm AN231K04-QUAD 3.3V development board.<sup>44</sup>

complex tasks such as amplify, integral, summation, filtering, comparison, and analog/digital or digital/analog conversion.<sup>45–47</sup>

The interface design of the realized fractional-order chaotic systems has two parts: (i) the part, which is defined as the dynamic equation, where it is upto entrance of the integrator likewise integer-order chaotic systems. This part is realized in FPAA1 CAB module for both the designs, e.g., Sprott type-H and Rössler. (ii) The fractional order part of the fractional-order dynamic system is realized by CAM blocks in FPAA2 CAB module. In this part, the used transfer function is generalized with (20).

The equation has nominator and denominator Laplace transformation with the power of 2 and 3, respectively. In the equation,  $GH_1$ ,  $GH_2$  and  $GH_3$  denote the gain of filters. Pole/Zero frequencies used in the primary and secondary bilinear filters are derived with the expressions of  $\omega_{z1}$ ,  $\omega_{z2}$ ,  $\omega_{p1}$ ,  $\omega_{p2}$  and  $\omega_{p3}$ . The low-pass filter frequency is obtained from the expression of  $\omega_{p0}$ . Table 3 gives the zero/pole frequencies along with low-pass filter frequency for fraction order of 0.9. The FPAA implementation of (20) is realized using the Anadigm Designer 2 software.<sup>48,49</sup> Even though Ref. 49 looks quiet similar to the work done here, there are some remarkable

Table 3. Chaotic attractors of the fractional-order system using the Charef method.

CAM	Filter Type	$f_z$	$f_p$	$G_H$
Bilinear1	Pole zero filter	$f_{z1} = 0.208$ Hz	$f_{p1} = 0.00206$ Hz	$G_{H1} = 10$
Bilinear2	Pole zero filter	$f_{z2} = 37.71$ Hz	$f_{p2} = 0.346$ Hz	$G_{H2} = 10$
Bilinear3	Pole zero filter	$f_{z3} = 57.87$ Hz		$G_{H3} = 6.23$

differences in between. In this paper, we are able simulate different fraction order, give simulation results that encapsulate comparative analysis of the fraction order where dynamic systems' phase-space portrait can be observed. Moreover, this paper offers more practical and implementable way of conducting experimental studies: the advantage of our design using fewer CAB block is that it utilizes circuit components more efficiently, i.e., requires less power.

$$T(s) = \frac{G_{H1}(w_{z1} + s)}{(w_{p1} + s)} \cdot \frac{G_{H2}(w_{z2} + s)}{(w_{p2} + s)} \cdot \frac{w_0 G_{H3}}{w_0 + s} \tag{20}$$

$$\begin{aligned} T(s) &= \frac{G_{H1}(w_{z1} + s)}{(w_{p1} + s)} \cdot \frac{G_{H2}(w_{z2} + s)}{(w_{p2} + s)} \cdot \frac{w_0 G_{H3}}{w_0 + s} \\ &= \frac{\left(1 + \frac{s}{1.29}\right) \left(1 + \frac{s}{215.18}\right)}{\left(1 + \frac{s}{0.0129}\right) \left(1 + \frac{s}{2.15}\right) \left(1 + \frac{s}{358.94}\right)} \\ w_{p1} &= \frac{1}{\tau_1}, \quad w_{p2} = \frac{1}{\tau_2}, \quad w_0 = \frac{1}{\tau_3} \end{aligned}$$

For the fractional order  $q = 0.9$ , transfer function is obtained with (17). With the transfer function expressed with (20), the pole frequencies,  $f_{p0}, f_{p1}$  and  $f_{p2}$ , zero frequencies,  $f_{z1}$  and  $f_{z2}$ , and gains,  $G_{H1}, G_{H2}$  and  $G_{H3}$ , are calculated as follows:

$$\begin{aligned} w_{p1} &= \frac{1}{\tau_1} = 2\pi f_{p1} = (ab)^1 ap_0, \quad f_{p1} = 0.00206 \text{ Hz}, \\ w_{p2} &= \frac{1}{\tau_2} = 2\pi f_{p2} = (ab)^2 ap_0, \quad f_{p2} = 0.34600 \text{ Hz}, \\ w_{p0} &= \frac{1}{\tau_3} = 2\pi f_{p0} = (ab)^3 ap_0, \quad f_{p0} = 57.8700 \text{ Hz}. \\ \\ w_{z1} &= 2\pi f_{z1} = (ab)^1 p_0, \quad f_{z1} = 0.208 \text{ Hz}, \\ w_{z2} &= 2\pi f_{z2} = (ab)^2 p_0, \quad f_{z2} = 37.71 \text{ Hz}, \\ G_{H3} &= (1/p_T^\alpha) = (1/0.01^{0.9}) = 6.23. \end{aligned}$$

The first-order pole and zero frequencies calculated above are designed in CAM configuration as FilterBilinear, as shown in Fig. 5. According to this, first bilinear filter zero, and pole frequencies, and high frequency gain are designed in FilterBilinear CAM block, respectively, as  $f_{z1} = 0.208 \text{ Hz}$ ,  $f_{p1} = 0.00206 \text{ Hz}$ , and  $G_{H1} = 1.0$ .

Moreover, the second-order pole and zero frequencies given with Fig. 6 are designed in CAM configuration as FilterBilinear. According to this, second bilinear filter zero, and pole frequencies, and high frequency gain are designed in FilterBilinear CAM block, respectively, as  $f_{z2} = 37.71 \text{ Hz}$ ,  $f_{p2} = 0.346 \text{ Hz}$ , and  $G_{H2} = 1.0$ .

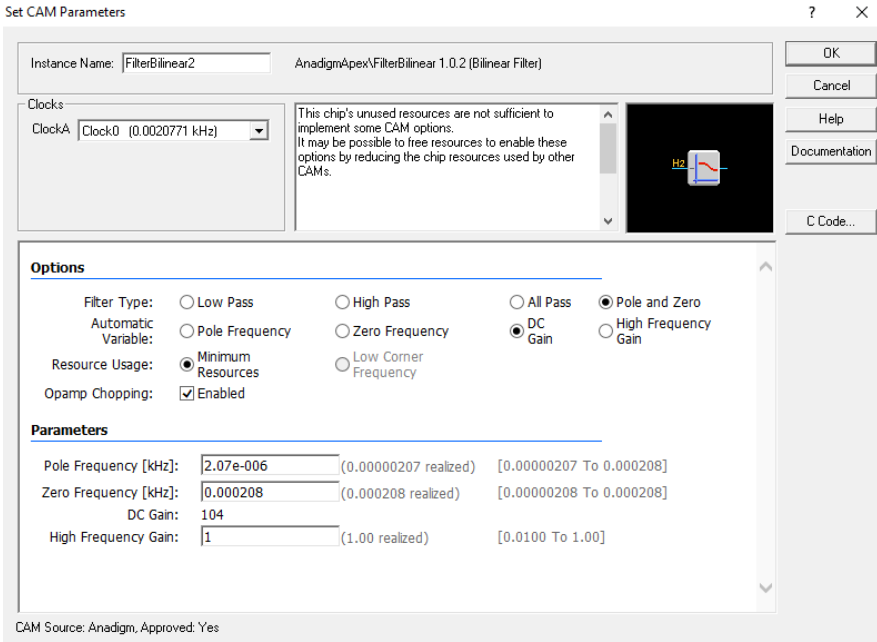


Fig. 5. CAM parameters of the first pole/zero bilinear filter.

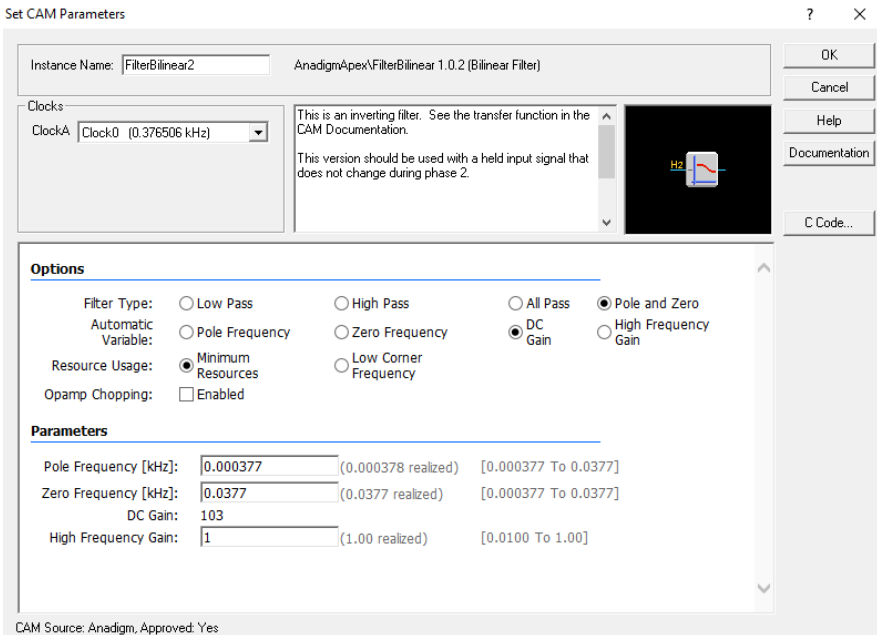


Fig. 6. CAM parameters of the second pole/zero bilinear filter.

J CIRCUIT SYST COMP Downloaded from www.worldscientific.com by Mr. Kenan ALTUN on 06/18/21. Re-use and distribution is strictly not permitted, except for Open Access articles.



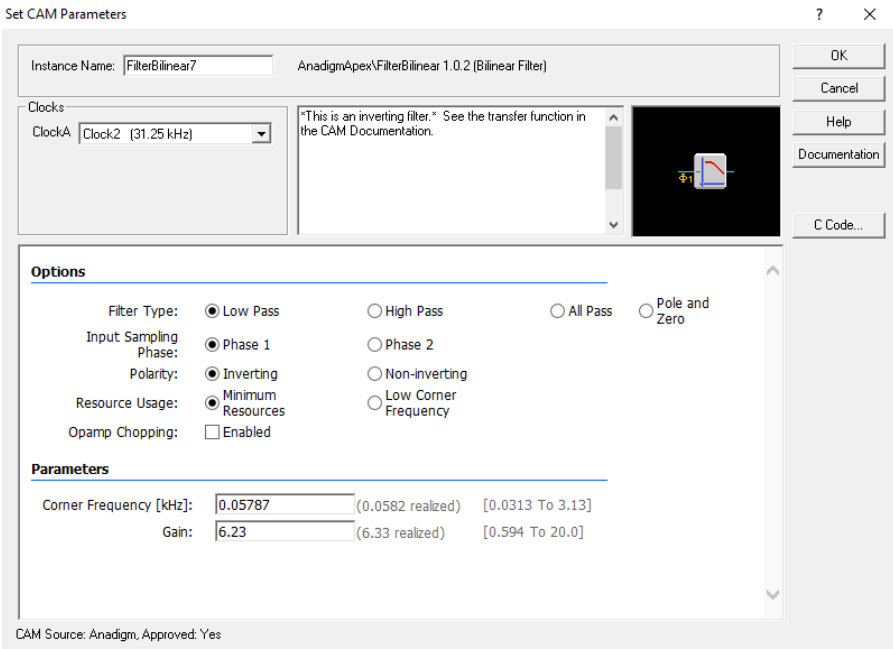


Fig. 7. CAM parameters of the third pole/zero bilinear filter.

Finally, 3rd multiplier of the transfer function given in (20) designed as a low-pass filter using CAM configuration, as shown in Fig. 7. According to this, low-pass filter cutting frequency is designed in FilterBilinear CAM as  $f_0 = 57.87$  Hz and  $G_{H3} = 6.23$ .

The FPAA realization blocks of fractional-order chaotic systems are shown in Figs. 8 and 9. Table 4 represents the blocks and their usage purposes in the realization of FPAA.

After they are designed in software interface, the designs in Figs. 8 and 9 are embedded in FPAA development board. The input and output information signals are experimentally measured from FPAA development board I/O terminals using digital oscilloscopes.

Figure 10 gives the Rössler chaotic system phase space representations for (a)  $q = 0.94$  and (b)  $q = 0.98$ . Figure 11 gives the  $x-y$ ,  $x-z$ ,  $y-z$  Sprott type-H chaotic system phase space representations for (a)  $q = 0.89$  and (b)  $q = 0.91$ .

It should be observed that the outcomes of the simulations and experimental studies show similarities. With the proposed design method, the fractional-order chaotic system’s analog-based fractional-order implementation is carried out. The study realized by using the FPAA structures represents the fractional-order real system behavior for nonlinear dynamic systems instead of integer order approximated results.

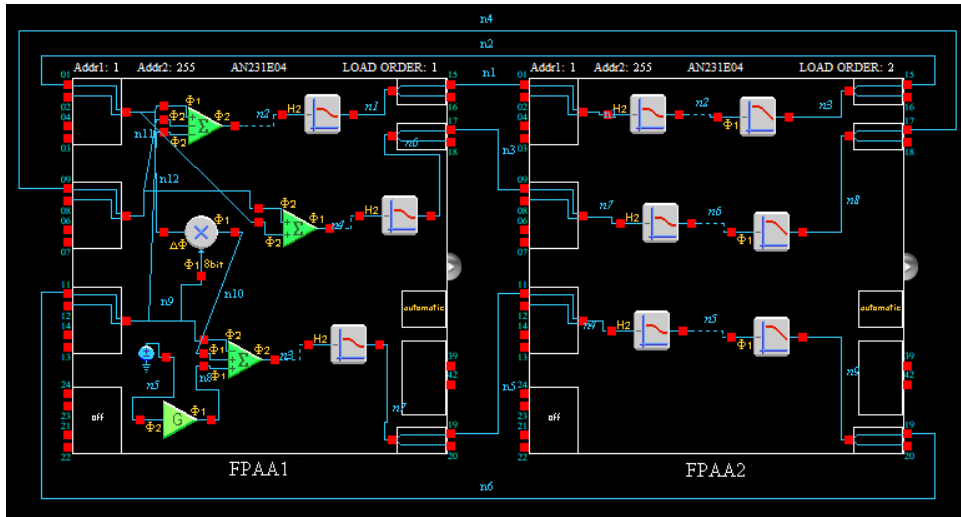


Fig. 8. FPAA implementation of proposed fractional-order chaotic system: Rössler chaotic generator and first pole-zero bilinear filter are presented in FPAA1, second pole-zero bilinear filter and third low pass filter are presented in FPAA2.

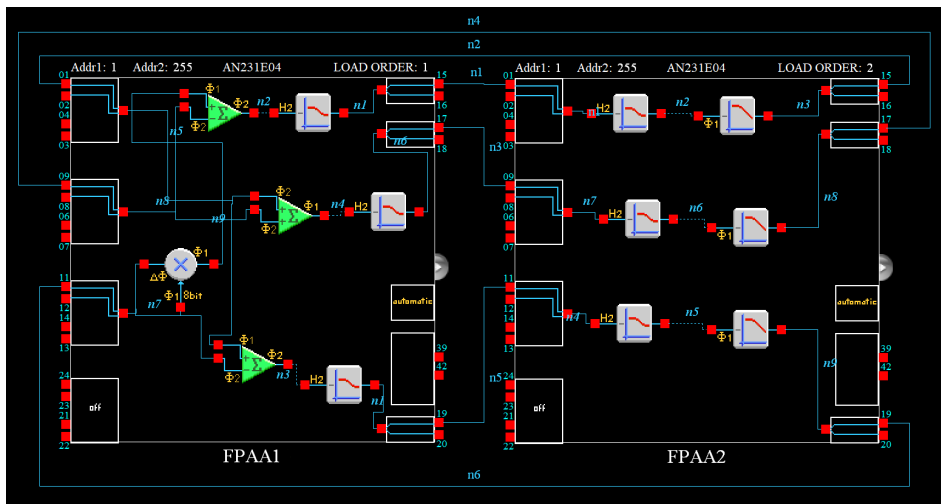
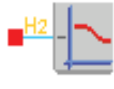
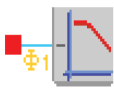
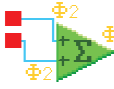





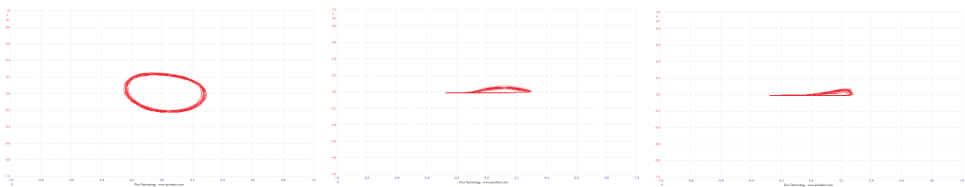
Fig. 9. FPAA implementation of proposed fractional-order chaotic system: Sprott type-H chaotic generator and first pole-zero bilinear filter are presented in FPAA1, second pole-zero bilinear filter and third low pass filter are presented in FPAA2.

With the help of this method, the performance observation of control system models can be realistically completed with high accuracy.

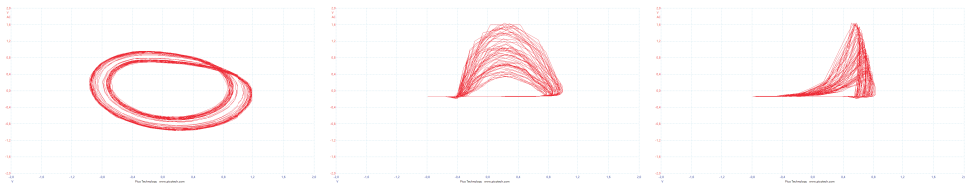
In this study, embedded system implementation of the fractional-order analog-based systems is realized. In Figs. 10 and 11, obtained results of the experimental

Table 4. FPAA realization blocks used in experimental study.

FPAA Realization Blocks		
FILTERBILINEAR BLOCK		FILTERBILINEAR blocks work as an creates pole and zero filter configuration by using Laplace transforms in FPAA1 and FPAA2.
FILTERBILINEAR BLOCK		FILTERBILINEAR blocks work as an creates low pass filter configuration by using Laplace transforms in FPAA2.
SUMDIFF BLOCK		SUMDIFF block creates a half cycle summing up to four inputs block in FPAA1.
MULTIPLIER WAVE BLOCK		MULTIPLIER WAVE BLOCK creates a multiplier in FPAA1.
GAINHALF BLOCK		GAINHALF BLOCK creates a half cycle gain stage in FPAA1.
DC VOLTAGE SOURCE BLOCK		DC VOLTAGE SOURCE block provides constant values in FPAA1.



(a)



(b)

Fig. 10. Rössler chaotic phase portrait; (a)  $x-y$ ,  $x-z$ ,  $y-z$  for  $q_1 = q_2 = q_3 = 0.94$ , (b)  $x-y$ ,  $x-z$ ,  $y-z$  for  $q_1 = q_2 = q_3 = 0.98$ .

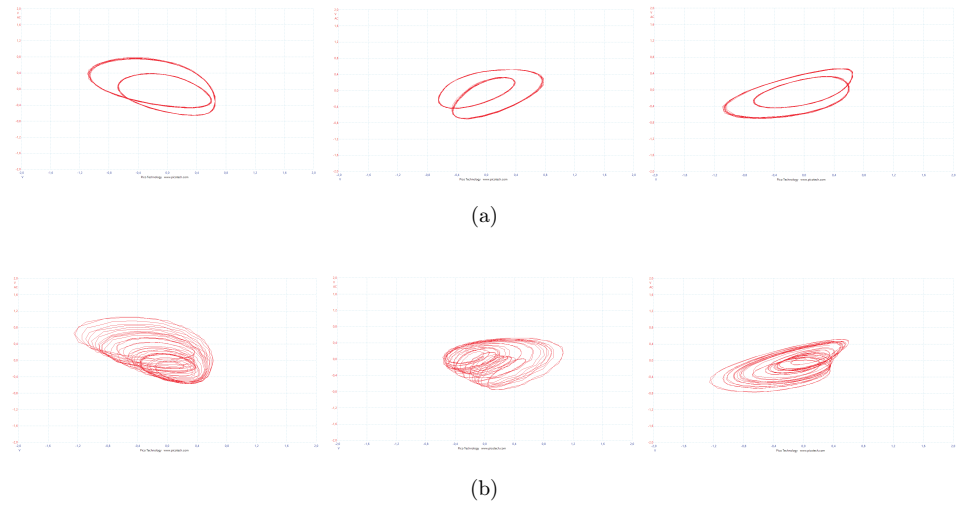


Fig. 11. Sprott type-H chaotic phase portrait; (a)  $x-y$ ,  $x-z$ ,  $y-z$  for  $q_1 = q_2 = q_3 = 0.89$  and (b)  $x-y$ ,  $x-z$ ,  $y-zq_1 = q_2 = q_3 = 0.91$ .

study, phase portraits of fractional-order Rössler and Sprott  $h$  oscillators are given. When the phase portraits of fractional-order oscillators are compared with the phase portraits of integer-order oscillators, it is observed that the fractional-order systems exhibit hyper chaos behavior. In order for the dynamic systems to exhibit hyper chaos behavior, they must have at least 4D or fractional order chaotic equation structure. This situation causes an increase in the number of potential channels in the chaotic based communication systems. Increasing the number of channels in the communication system results in increased system complexity. Thus, with the increase in the number of channels in the transmitter circuit of the communication system, the number of unpredictable channels increases. This situation decreases the possibility of external intervention to the communication channel and increases the reliability of the communication system.

### 5. Conclusion

In this study, the analog-based implementation of fractional order chaotic systems was presented. In Rössler and Sprott type-H chaos systems, variety of transfer functions was obtained for the different values of fractional orders, and was simulated using MATLAB Simulink. The transfer functions of chaotic systems were realized using the Charef approximation method. The fractional orders in the transfer functions that exhibit chaos conditions were numerically determined using the eigenvalues of chaos system. With the simulation studies, the state of chaos at fractional degrees calculated for dynamical systems was tested. For fractional degrees in theoretically calculated chaos conditions, the chaos state of dynamic

systems was simulated. The data obtained from the theoretical and simulation results were also confirmed with experimental results. The system design and experimental realization of fractional-order chaotic system were completed using analog-based development board of AN231K04-QUAD. In the FPAA CAB design of transfer functions, BilinearFilter CAM modules was utilized. This paper showed the implementation of fractional-order chaotic systems using FPAA. The experimental observations of the attractors generated by the FPAA-based implementation of both Rössler and Sprott type-H have been demonstrated. These structures can be used in real-time design of many systems such as reliable communication systems and control systems. It was observed that the outcomes of experimental studies matched with the simulation results. As a future work, the proposed method will be integrated into coherent chaotic communication systems, in which synchronization with different fractional order or integer order chaotic system is a challenging issue, to increase the complexity, and thereby communication security.

## References

1. P. Holmes, Celestial mechanics, dynamical-systems theory and “chaos”, *Phys. Rep.* **193** (3) (1990) 137–163.
2. E. Ott, C. Grebogi and J. A. Yorke, Controlling chaos, *Phys. Rev. Lett.* **64**(11) (1990) 1196.
3. E. N. Lorenz, Deterministic nonperiodic flow, *J. Atmos. Sci.* **20** (1963) 130–141.
4. H. O. Peitgen, H. Jürgens and D. Saupe, *Chaos and Fractals: New Frontiers of Science* (Springer Science Business Media, New York, 2004), p. 864.
5. I. Petras and D. Bednarova, Fractional-order chaotic systems, *2009 IEEE Conf. Emerging Technologies Factory Automation*, Mallorca, 2009, pp. 1–8.
6. K. Nishimoto, *Fractional Calculus: Integrations and Differentiations of Arbitrary Order*, Vol. 4 (Descartes Press, Koriyama, 1984).
7. K. Oldham and J. Spanier, *The Fractional Calculus Theory and Applications of Differentiation and Integration to Arbitrary Order* (Elsevier, 1974), p. 322.
8. A. Oustaloup, F. Levron, B. Mathieu and F. M. Nanot, Frequency-band complex non-integer differentiator: characterization and synthesis, *IEEE Trans. Circuits Syst. I, Fundamental Theory Appl.* **47** (2000) 25–39.
9. Y. Jin, Y. Q. Chen and D. Xue, Time-constant robust analysis of a fractional order [proportional derivative] controller, *IEET Control Theory Appl.* **5** (2011) 164–172.
10. H. Zhang, X. Y. Wang and X. H. Lin, Stability and control of fractional chaotic complex networks with mixed interval uncertainties, *Asian J. Control* **19** (2017) 106–115.
11. I. Petráš, *Fractional-Order Nonlinear Systems: Modeling, Analysis and Simulation* (Springer-Verlag, Berlin Heidelberg, 2011), p. 218.
12. U. N. Katugampola, A new approach to generalized fractional derivatives, *Bull. Math. Anal. Appl.* **6** (2014) 1–15.
13. M. A. Herzallah, Notes on some fractional calculus operators and their properties, *J. Fract. Calc. Appl.* **5** (2014) 1–10.
14. A. Atangana and J. F. Gómez-Aguilar, Fractional derivatives with no-index law property: application to chaos and statistics, *Chaos, Solitons Fractals* **114** (2018) 516–535.

15. S. Ma, J. Zheng and Y. Li, Chaos control and synchronization of a new fractional order chaotic system, *J. Inform. Comput. Sci.* **11** (2014) 3469–3479.
16. K. Shah, F. Jarad and T. Abdeljawad, On a nonlinear fractional order model of dengue fever disease under caputo-fabrizio derivative, *Alexandria Eng. J.* **59** (2020) 2305–2313.
17. J. E. S. Pérez, J. F. Gómez-Aguilar, D. Baleanu and F. Tchier, Chaotic attractors with fractional conformable derivatives in the Liouville-Caputo sense and its dynamical behaviors, *Entropy* **20** (2018) 384.
18. L. F. Ávalos-Ruiz, C. J. Zúñiga-Aguilar, J. F. Gómez-Aguilar, R. F. Escobar-Jiménez and H. M. Romero-Ugalde, FPGA implementation and control of chaotic systems involving the variable-order fractional operator with Mittag-Leffler law, *Chaos, Solitons Fractals* **115** (2018) 177–189.
19. A. Coronel-Escamilla, J. F. Gómez-Aguilar, L. Torres, R. F. Escobar-Jiménez and M. Valtierra-Rodríguez, Synchronization of chaotic systems involving fractional operators of Liouville-Caputo type with variable-order, *Physica A, Stat. Mech. Appl.* **487** (2017) 1–21.
20. I. Podlubny, *An Introduction to Fractional Derivatives, Fractional Differential Equations, to Methods of their Solution and Some of their Applications* (Academic Press, 1998), p. 340.
21. M. F. Tolba, L. A. Said, A. H. Madian and A. G. Radwan, Fpga implementation of the fractional order integrator/differentiator: Two approaches and applications, *IEEE Trans. Circuits Syst. I, Regular Papers* **66** (2018) 1484–1495.
22. P. Gora and A. Boyarsku, Why computers like Lebesgue measure, *Comput. Math. Appl.* **16** (1998) 321–329.
23. Z. Galias, The dangers of rounding errors for simulations and analysis of nonlinear circuits and systems and how to avoid them, *IEEE Circuits Syst. Mag.* **13** (2013) 35–52.
24. S. Li, G. Chen and X. Mou, On The dynamical degradation of digital piecewise linear chaotic maps, *Int. J. Bifurcation Chaos* **15** (2005) 3119–3151.
25. S. H. M. Kilbas and A. J. J. Trujillo, *Theory and Applications of Fractional Differential Equations* (Elsevier, 2006), p. 540.
26. K. S. Miller and B. Ross, *An Introduction to the Fractional Calculus and Fractional Differential Equations* (Wiley, New York, 1993) p. 363.
27. R. Caponetto, G. Dongola, G. Maione and A. Pisano, Integrated technology fractional order proportional-integral-derivative design, *J. Vib. Control* **20** (2014) 1066–1075.
28. T. T. Hartley and C. F. Lorenzo, Dynamics and control of initialized fractional-order systems, *Nonlinear Dyn.* **29** (2002) 201–233.
29. M. H. Sabzalian, A. Mohammadzadeh, S. Lin, and W. Zhang, Robust fuzzy control for fractional-order systems with estimated fraction-order, *Nonlinear Dyn.* **98** (2019) 2375–2385.
30. Y. Luo, and Y. Chen, *Fractional Order Motion Controls* (Wiley Online Library, 2012), p. 454.
31. B. Ross, The development of fractional calculus, *Historia Math.* **4** (1977) 75–89.
32. A. Charef, H. Sun, Y. Tsao and B. Onaral, Fractal system as represented by singularity function, *IEEE Trans. Automatic Control* **37** (1992) 1465–1470.
33. A. Loverro, Fractional calculus: History, definitions and applications for the engineer, Rapport technique, *Univeristy of Notre Dame: Department of Aerospace and Mechanical Engineering*, Vol. 1–28 (2004).
34. D. Matignon, Stability results for fractional differential equations with applications to control processing, *Computational Engineering in Systems Applications*, Vol. 2 (1996), pp. 963–968.
35. O. E. RöSSLer, An equation for continuous chaos, *Phys. Lett. A* **57** (1976) 397–398.

36. J. C. Sprott, Some simple chaotic flows, *Phys. Rev. E* **50** (1994) R647.
37. D. R. D'mello and P. G. Gulak, Design approaches to field-programmable analog integrated circuits, in: Field-Programmable Analog Arrays, *Analog Integr. Circuits Signal Process.* **17** (1998) 7–34.
38. T. Roberts, Using field-programmable analog to build adaptable rfid readers, *RF and Microwave Technol. Design Eng.* **27** (2004) 44–48.
39. S. Shah, J. Hasler, S. Kim, I. Lal, M. Kagle and M. Collins, Demonstration of a remote fpaa system for research and education, *IEEE Int. Symp. Circuits and Systems (ISCAS)*, IEEE, 2016, pp. 1441–1441.
40. R. Kilic, Universal programmable chaos generator: Design and implementation issues, *Int. J. Bifurcation Chaos* **20** (2010) 419–435.
41. A. Riaz and M. Ali, Chaotic communications, their applications and advantages over traditional methods of Communication, *2008 6th Int. Symp. Communication Systems, Networks and Digital Signal Processing*, IEEE, 2008, pp. 21–24.
42. R. Sarahuja, V. Barcons, L. Balado and J. Figueras, Experimental test bench for mixed-signal circuits based on fpaa devices, *Proc. 18th Conf. Design of Circuits and Integrated Systems*, 2003, pp. 344–349.
43. T. R. Balen, A. Q. Andrade, F. Azais, M. Lubaszewski and M. Renovell, Applying the oscillation test strategy to fpaa's configurable analog blocks, *J. Electronic Testing* **21** (2005) 135–146.
44. Anadigm, <https://anadigm.com/doc/UM231004-K001.pdf>, Accessed:2020-07-22.
45. C. Muñoz-Montero, L. V. García-Jiménez, L. A. Sánchez-Gaspariano, C. Sánchez-López, V. R. González-Díaz and E. Tlelo-Cuautle, New alternatives for analog implementation of fractional-order integrators, differentiators and pid controllers based on integer-order integrators, *Nonlinear Dyn.* **90** (2017) 241–256.
46. C. Muñoz-Montero, L. A. Sánchez-Gaspariano, C. Sánchez-López, V. R. González-Díaz and E. Tlelo-Cuautle, On the electronic realizations of fractional-order phase-lead-lag compensators with opamps and fpaas, *Fractional Order Control and Synchronization of Chaotic Systems* (Springer International Publishing, 2017), pp. 131–164.
47. T. J. Freeborn, B. Maundy and A. S. Elwakil, Field programmable analogue array implementation of fractional step filters, *IET Circuits, Devices Syst.* **4** (2010) 514–524.
48. E. Tlelo-Cuautle, A. D. Pano-Azucena, O. Guillén-Fernández and A. Silva-Juárez, *Analog/Digital Implementation of Fractional Order Chaotic Circuits and Applications* (Springer International Publishing, 2020), p. 212.
49. A. Silva-Juárez, E. Tlelo-Cuautle, L. G. de la Fraga and R. Li, FPAA-based implementation of fractional-order chaotic oscillators using first-order active filter blocks, *J. Adv. Res.* **25** (2020) 77–85.